

1 Article

# 2 **Combustion and Emission Enhancement of a Spark** 3 **Ignition Two-Stroke Cycle Engine Utilizing Internal** 4 **and External EGR Approach at Low-Load Operation**

5 **Amin Mahmoudzadeh Andwari** <sup>1,2,3\*</sup>, **Apostolos Pesyridis** <sup>1</sup>, **Vahid Esfahanian** <sup>2</sup>, **Mohd Farid**  
6 **Muhamad Said** <sup>3</sup>

7 <sup>1</sup> Centre for Advanced Powertrain and Fuels Research (CAPF), Department of Mechanical, Aerospace and  
8 Civil Engineering, Brunel University London, London UB8 3PH, UK; a.pesyridis@brunel.ac.uk

9 <sup>2</sup> Vehicle, Fuel and Environment Research Institute (VFERI), School of Mechanical Engineering, College of  
10 Engineering, University of Tehran, Tehran 1439956191, Iran; evahid@ut.ac.ir

11 <sup>3</sup> Automotive Development Centre (ADC), School of Mechanical Engineering, Faculty of Engineering,  
12 Universiti Teknologi Malaysia, 81310 Johor Bahru; mdfarid@utm.my

13

14 \* Correspondence: amin.mahmoudzadehandwari@brunel.ac.uk; Tel.: +44-(0)-1895-267901

15 Academic Editor: Prof.

16 Received: date; Accepted: date; Published: date

17 **Abstract:** Two-stroke cycle engines have always been prominent due to their distinctive advantage  
18 incorporating high power-to-weight ratio, however the drawbacks are poor combustion efficiency,  
19 fuel short-circuiting and excessive emission of uHC and CO. These problems are apparent at low-  
20 load and speed regions and are the major obstacle to their global acceptance. The deficiencies can  
21 be addressed by increasing the in-cylinder average charge temperature employing Exhaust Gas  
22 Recirculation (EGR). An experimental study is conducted to investigate the influence of utilizing  
23 EGR techniques, including Internal and External EGR, on combustion misfiring occurrence,  
24 combustion stability and exhaust emissions using a single cylinder two-stroke SI engine at idling,  
25 low and mid-load conditions. From the results, it is observed since the average in-cylinder charge  
26 temperature is increased, due to utilizing EGRs, engine's low and mid-load irregular combustions  
27 (misfire) and exhaust emissions are remarkably suppressed and almost all of misfire cycles  
28 eliminated depending on the percentage of EGRs. In terms of combustion stability, it is agreed in  
29 general the application of EGRs improves the cyclic variation of IMEP,  $P_{max}$  and CA10 compared to  
30 conventional operation. However, applying Ex-EGR compared to In-EGR will deteriorate cyclic  
31 variability of IMEP and CA10.

32 **Keywords:** Two-Stroke Cycle Engine; Misfire; Cyclic Variation; Internal EGR; External EGR;  
33 Exhaust Emissions

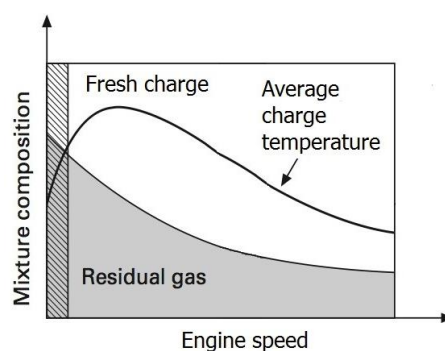
34

## 35 **1. Introduction**

36 Since the fossil fuel resources are finite and the effect of greenhouse issue, Internal Combustion  
37 Engines (ICEs) having high thermal efficiency and lower exhaust gas emission have been always at  
38 the point of interest for IEC's research and development scientists [1-3]. There are some irrefutable  
39 advantages for two-stroke cycle engines, comprising light weight, simple construction, less  
40 components, cheap to manufacturing and the potential to pack almost twice the power-density than  
41 that of a four-stroke engine having similar capacity. This makes them unique among any other ICE  
42 types [4-8]. Numerous substantial research works were conducted to tackle two-stroke engines main  
43 drawback, which is high level of unburned hydrocarbons (uHC) emissions, caused by unstable  
44 running operation combined with incomplete combustion known as misfire cycle, especially at light

45 load [9-14]. Cycle-to-cycle variation at low and mid-load has long been known as one of the  
 46 drawbacks in two-stroke cycle engines. This cyclic variation is attributed to lower average charge  
 47 temperature of the cylinder, as at low-speed and low-load, the amount of energy released per each  
 48 combustion cycle is too low to maintain the next combustion cycle temperature to be continued  
 49 without misfiring [15-21]. Fig. 1 represents the typical relationship between the average charge  
 50 temperature at the start of compression stroke (exhaust port closure temperature,  $T_{epc}$ ) and quantity  
 51 of fresh charge and residual gas. It explains the effect of engine speed in conjunction with average  
 52 charge temperature for the reference conventional two-stroke cycle engine [22-25].

53 As can be seen from Fig.1 that the  $T_{epc}$  is low when the engine is run at low-speed (hatched region)  
 54 and high-speed. A high magnitude of  $T_{epc}$  can be reached when the engine speed is beyond the mid-  
 55 speed but not at engine top-end speed. The reasons for having lower  $T_{epc}$  at engine high speed are  
 56 attributed to lower amount of available residual gases and shorter available time for mixing of fresh  
 57 charge and residual gases. It has been found that depending on the engine speed, load and level of  
 58 Exhaust Gas Recirculation (EGR), it is possible to increase the  $T_{epc}$  in a two-stroke engine due to the  
 59 mixing of unburned gas introduced into the cylinder and hot residual gas (burned gas) [26-30].  
 60



61  
 62 **Figure 1.** Variation of average charge temperature at the start of compression ( $T_{epc}$ ), quantity of fresh  
 63 charge and residual gas against engine speed in a typical two-stroke cycle engine [25]

## 64 2. Influence of EGR Application

65 Exhaust port closure temperature ( $T_{epc}$ ) should be sufficiently high to achieve a complete  
 66 combustion at the end of the compression stroke via spark plus ignition. The usage of EGR will result  
 67 in a higher gas temperature regime throughout the compression process, which in turn speeds up the  
 68 chemical reactions which will lead to the start of combustion of homogeneously mixed fuel and air  
 69 mixtures [31-35]. These requirements can be realized by recycling or trapping the burned gases within  
 70 the cylinder, which the former is called External EGR (Ex-EGR) and the latter is called Internal EGR  
 71 (In-EGR), respectively. The effect of using EGR on the engine combustion and engine performance  
 72 has been well studied by many of researchers over a wide range of all ICE types. In general, four  
 73 major effects of utilizing EGR on combustion characteristics can be explained as follows [7, 36-40]:  
 74

- 75 1) **Charge Heating Effect**-Hot burned gases increase the temperature of the intake charge.
- 76 2) **Heat Capacity Effect**-Species in the hot burned gases including carbon dioxide ( $\text{CO}_2$ ) and  
 77 water vapor ( $\text{H}_2\text{O}$ ) have higher value of heat capacity.
- 78 3) **Dilution Effect**-lower air/oxygen concentration due to substitution of inert gases existed in  
 79 the hot burned gases.
- 80 4) **Chemical Effect**-Hot burned gases consist of some activated radical species, which expedite  
 81 the chemical reaction of combustion.

82  
 83 This objective of the experimental work is to investigate the influence of internal as well as  
 84 external EGR on the combustion improvement of a typical spark ignition two-stroke cycle engine.  
 85 The parameters of interest are: i) combustion cyclic variability, ii) misfire occurrence and iii) exhaust  
 86 emissions.

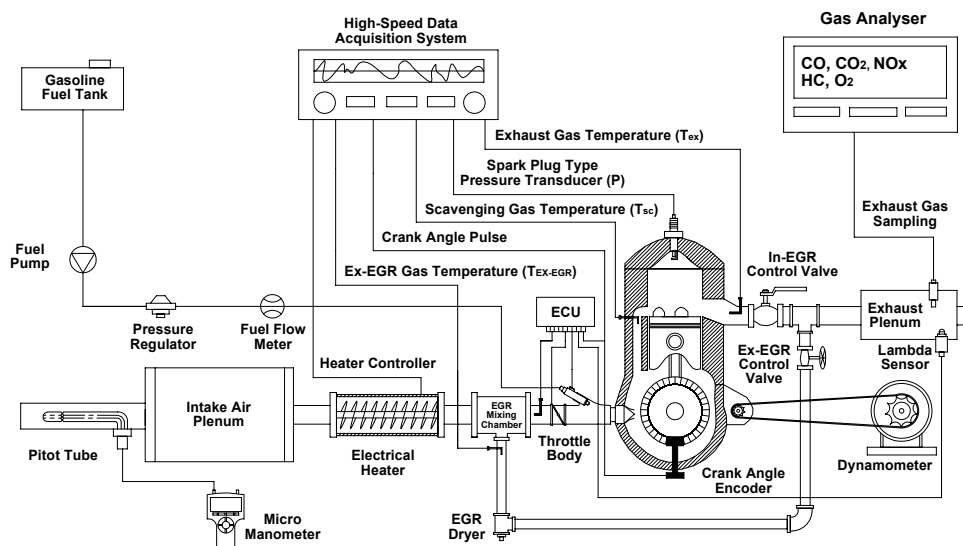
### 87 3. Engine Specifications

88 A single cylinder two-stroke, naturally aspirated, liquid-cooled engine is modified to prepare it  
89 as a test engine for this work. The specifications are in Table 1.

90 **Table 1.** Experimental engine specifications

Engine Type	Single Cylinder 2-Stroke Case Reed Valve
Bore × Stroke	59 × 54.5 (mm)
Displacement	149 (cm <sup>3</sup> )
Scavenging Type	Schnurle (Loop Scavenging)
Scavenging Port Timing	117.5 CAD a/bTDC
Exhaust Port Timing	82.5 CAD a/bTDC
Exhaust System	Expansion Chamber
Compression Ratio	8.5:1
Cooling System	Liquid Cooled
Fuel Supply System	Port Fuel Injection
Scavenging Coefficients	$K_0 = 0.02904, K_1 = -1.0508, K_2 = -0.34226$

91 It is equipped with an electronically fuel injection system to provide appropriate air-to-fuel ratio  
92 (AFR). A closed loop lambda control system is included to ensure the AFR will be precisely set in  
93 compliance with the engine's ECU settings. Intake air box and Pitot tube are employed to measure  
94 the engine's air consumption. The exhaust piping architecture is developed to be able to utilize some  
95 portion of the combustion products to be recycled to part of the intake mixture for the next charge.  
96 Combustion burned gases inside of the combustion chamber can be retained in the combustion  
97 chamber by means of exhaust port area restriction. These high temperature burned gases will mix  
98 with the new incoming fresh air and fuel charge resulting higher temperature and pressure at the  
99 moment after completion of the scavenging process. This strategy of the burned gas utilization is  
100 known as Internal EGR (In-EGR). Here one ball type valve (diameter 38 mm) is mounted in the  
101 exhaust pipe where it is 50 mm away from engine's exhausting port downstream side. The valve is  
102 designed to restrict the exhaust port area from 0-90%. The setup is in Fig. 2.  
103  
104



105

106

**Figure 2.** Schematic view of experimental test rig setup

107 A T-joint connection of 25 mm diameter is fitted immediately after the In-EGR to induce a fraction  
108 of the exhaust gases from the exhaust pipe into the intake runner. This method of burned gas  
109 utilization is known as External EGR (Ex-EGR). The technique will not only result in higher intake  
110 charge temperature but will also produce different intake charge composition. The burned gases due

111 to Ex-EGR will be mixed with the intake air via one mixing chamber called Ex-EGR mixing chamber.  
 112 A gate type valve is fitted onto the induction line connecting to the mixing chamber. The induction  
 113 line is completely insulated to minimize both the convection and the conduction heat transfer losses.

#### 114 4. Instrumentation and Test Procedure

115 With reference to Fig. 2, several K-type thermocouples ( $\pm 1$  °C accuracy) are fitted at strategic  
 116 locations to measure for  $T_{ex}$ ,  $T_{in}$  and  $T_{sc}$ , (engine exhaust gas temperature, intake gas temperature and  
 117 transfer port gas temperature). One piezoelectric pressure transducer (KISTLER 6117B) is used, in  
 118 replacement of the engine spark plug, to record for combustion pressure history. The engine  
 119 crankshaft is coupled to one crank angle encoder (KISTLER 2613B) to measure for engine crank angle  
 120 rotation (CAD) with 0.2 Degree of resolution. A high-speed data acquisition system (DEWE5000),  
 121 equipped with software (DEWESoft and DEWECa), is used for data logging. The engine is connected  
 122 to an eddy-current brake dynamometer (30 kW MAGTROL) via chain and sprockets. Engine fuel  
 123 consumption is measured using an on-line type fuel flow sensor (ONO SOKKI FP-2240HA). As for  
 124 engine emission, one portable exhaust gas analyzer (EMS 5002) is employed to induce a minute  
 125 concentration of the HC, CO<sub>2</sub> NO<sub>x</sub>, O<sub>2</sub> and CO<sub>2</sub>. Gasoline 95 (octane rating 95) is used throughout the  
 126 entire of experimental program.

#### 127 5. In-Cylinder Gas Thermodynamic and Scavenging Model

128 It is assumed that the scavenging process in the engine combustion chamber will follow an  
 129 idealized Isothermal Perfect-Mixing model. According to this model, as the fresh charge enters the  
 130 cylinder it will mix instantaneously with the cylinder charge to form a homogeneous mixture at a  
 131 constant volume, pressure, and temperature. The cylinder walls are adiabatic, the entering charge  
 132 has the thermodynamic properties of the ambient as well as the two gases involved follow the ideal  
 133 gas law and have the same molecular weights with identical and constant specific heats [15, 35, 39,  
 134 41]. The scavenging efficiency ( $\eta_{sc}$ ) is exponentially correlated with the corrected delivery ratio ( $L$ ) in  
 135 terms of a nonlinear second order semi-empirical equation as explained in Eq. 1.

$$137 \quad \eta_{sc} = 1 - \text{Exp}(k_0 + k_1 L + k_2 L^2) \quad (1)$$

138  
 139 Where  $k_0$ ,  $k_1$ ,  $k_2$  are scavenging coefficients which represent several types of transfer port  
 140 geometry. The value of each of these coefficients for loop scavenging having five transfer ports is  
 141 represented in Table 1 [10, 42].  $L$  is the corrected delivery ratio and can be found from Eq. 2.

$$143 \quad L = \frac{M_{del}}{M_{tr}} = \frac{m_{Air} \times \frac{60}{N_s} \left[ 1 + \frac{1}{AFR} \right]}{\left[ \frac{P_{epc} \times V_{epc}}{R \times T_{epc}} \right]} \quad (2)$$

144 Where  $m_{Air}$  is engine intake mass flow rate and  $R$  is specific gas constant.  $P_{epc}$ ,  $V_{epc}$  and  $T_{epc}$  are  
 145 pressure, volume and temperature of the engine cylinder gas at the moment when the exhaust port  
 146 is closed (start of the effective compression).  $N_s$  is engine speed in rpm and AFR is engine air-to-fuel  
 147 ratio. When the exhaust port is fully closed by piston (start of effective compression) enthalpy balance  
 148 equation (Eq. 3) is governed [35, 41, 43, 44] in order to estimate the  $T_{epc}$ .

$$150 \quad M_{epc} \times T_{epc} \times Cp_{epc} = M_{sc} \times T_{sc} \times Cp_{sc} + M_r \times T_r \times Cp_r \quad (3)$$

$$152 \quad T_{epc} = \frac{M_{epc} \times \eta_{sc} \times T_{sc} \times Cp_{sc} + M_{epc} (1 - \eta_{sc}) T_r \times Cp_r}{M_{epc} \times Cp_{epc}} \quad (4)$$

153

154 By assuming equal specific heats for all constituents of the in-cylinder charge [6, 15, 18, 23] (i.e.  
 155 exhaust port closure mixture, scavenging gas and residual gas;  $Cp_{epc} = Cp_{sc} = Cp_r$ ), the  $T_{epc}$  is now  
 156 derive as Eq. 5:

$$158 T_{epc} = T_{sc}\eta_{sc} + T_r(1 - \eta_{sc}) \quad (5)$$

159  
 160 The residual gas temperature ( $T_r$ ) is estimated by averaging of the exhaust gas temperature ( $T_{ex}$ )  
 161 and the in-cylinder gas temperature at the exhaust port opening ( $T_{epo}$ ) (blow-down gas temperature)  
 162 as [39]:

$$164 T_r = \frac{T_{ex} + T_{epo}}{2} \quad (6)$$

165 Having assumed for adiabatic process during piston descending (expansion) [15, 39, 41],  $T_{epo}$  can  
 166 be estimated by Eq. 7.

$$168 T_{epo} = T_{max} \left[ \frac{P_{epo}}{P_{max}} \right]^{\frac{k-1}{k}} \quad (7)$$

169  
 170 Where  $T_{max}$  and  $P_{max}$  are data acquired from experimental work and  $k$  is polytropic exponent. The  
 171 exponent  $k = 1.32$  is assumed for the average specific heat capacity ratio of the mixture since quasi-  
 172 adiabatic process mostly governs the compression and expansion stroke in ICEs engine [15, 35, 39].  
 173 Therefore, Eq. 5 can be rewritten as Eq. 8:

$$175 \eta_{sc} = \frac{T_{epc} - T_r}{T_{sc} - T_r} \quad (8)$$

176  
 177 Finally  $T_{epc}$  is calculated by substitutive Eq. 8 into Eq. 1 and Eq. 2 respectively. Once  $T_{epc}$  is  
 178 specified, the  $\eta_{sc}$  can be estimated using Eq. 1. Consequently, the  $T_{epc}$  and  $\eta_{sc}$  are estimated by a  
 179 semi-empirical correlation, which is combined with the equation derived from experiment and the  
 180 enthalpy balance equation at the state of the exhaust port closure.

## 181 6. Estimation of In-EGR and Ex-EGR Rate

182 After completion of the scavenging process (i.e. closure of the exhaust port), some fractions of  
 183 the burned gas will remain in the combustion chamber. It is known as residual gas, wherein the  
 184 residual gas ratio ( $\gamma$ ) is quantified by Eq. 9.

$$186 \gamma = 1 - \eta_{sc} \quad (9)$$

187  
 188 Typically, in all ICEs, especially in two-stroke cycle engines employing conventional scavenging  
 189 technique, some small amounts of the residual gas are trapped in the combustion chamber  
 190 permanently. The residual gas can either be increased or decreased depending on the efficiency of  
 191 the scavenging process but it can never be removed completely [1, 41]. This fraction of the residual  
 192 gas, which is not removable, it called inherent residual gas ratio ( $\gamma_{inh}$ ). The  $\gamma_{inh}$  can be measured when  
 193 the engine without EGR (i.e. neither In-EGR nor Ex-EGR are applied). Applied residual gas ratio ( $\gamma_{ap}$ )  
 194 can be achieved when the engine is operated by means of either In-EGR or Ex-EGR. Hence Eq. 9 can  
 195 now be interpreted as follow [45-48]:

196  
 197 Normal operating condition (without In/Ex-EGR):

$$199 (\eta_{sc})_{inh} = 1 - Exp(k_0 + k_1 L_{inh} + k_2 L_{inh}^2) \quad (10)$$

200

$$\gamma_{inh} = 1 - (\eta_{sc})_{inh} \quad (11)$$

202

203 Operating condition with In/Ex-EGR:

$$(\eta_{sc})_{ap} = 1 - \text{Exp}(k_0 + k_1 L_{ap} + k_2 L_{ap}^2) \quad (12)$$

$$\gamma_{ap} = 1 - (\eta_{sc})_{ap} \quad (13)$$

206

207 After determining the residual gas ratio ( $\gamma$ ) in both applied and inherent conditions, the In-EGR  
208 and Ex-EGR rates can be estimated as follows [49-53]:

$$\text{In-EGR} = (\gamma_{ap} - \gamma_{inh}) \times 100\% \quad (14)$$

$$\text{Ex-EGR} = (\gamma_{ap} - \gamma_{inh}) \times 100\% \quad (15)$$

211

## 212 7. Results and Discussions

### 213 7.1 Idling, Low-Load and Mid-Load Misfiring Improvement

214 In order to investigate for the engine's combustion stability, misfire index is taken into  
215 consideration. This parameter is quantified between one and zero, representing misfire and ideal  
216 combustion respectively. In the combustion chamber, it is assumed that a misfire cycle will occur  
217 when the indicated mean effective pressure (IMEP) of the combustion cycle is zero.

218 The engine is run at three speeds and loads with respect to several amounts of both internal and  
219 external EGR, as specified in Table 2. As such, three speeds and loads are considered to evaluate the  
220 engine's misfire improvement i.e. 1000 rpm (IMEP = 1 bar; Idling), 2000 rpm (IMEP = 1.5 bar; low-  
221 load) and 3000 rpm (IMEP = 2.1 bar; mid-load). All data are recorded for 120 consecutive cycles of the  
222 engine operation.

223

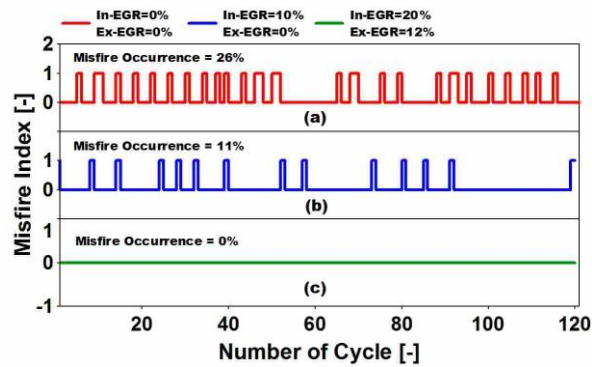
**Table 2.** Operating conditions of the engine for misfiring test

Parameters	Ranges		
	1000 Idling	2000 Low-Load	3000 Mid-Load
Speed [rpm] $\pm 50$	1000 Idling	2000 Low-Load	3000 Mid-Load
Fuel [-]	Gasoline 95	Gasoline 95	Gasoline 95
IMEP [bar] $\pm 0.1$	1.0	1.5	2.1
$T_{epc}$ [K] $\pm 1$	420	431	451
AFR [-] $\pm 0.5$	15	14.5	13.5
In-EGR [%] $\pm 1$	20	14	10
Ex-EGR [%] $\pm 1$	12	7	4

224

225 Fig. 3 shows the number of misfire occurrence when the engine is operated at 1000 rpm (idling),  
226 at various settings of the EGRs. When the engine is run at a normal condition (without In-EGR or Ex-  
227 EGR), 31 cycles out of 120 consecutive cycles are observed as misfired, meaning that the misfire  
228 occurrence is almost 26 % (refer marking (a)). On the other hand, marking (b) shows by applying just  
229 10% of In-EGR, the misfire occurrence has reduced to 11% i.e. 13 misfired cycles. All of the misfired  
230 cycles can be completely eliminated when both In-EGR and Ex-EGR are set at 20% and 12%,  
231 respectively as shown by marking (c). The results imply that the EGR utilization will improve the  
232 engine combustion stability leading to the reduction in the incomplete combustion (misfiring) at  
233 idling condition.

234



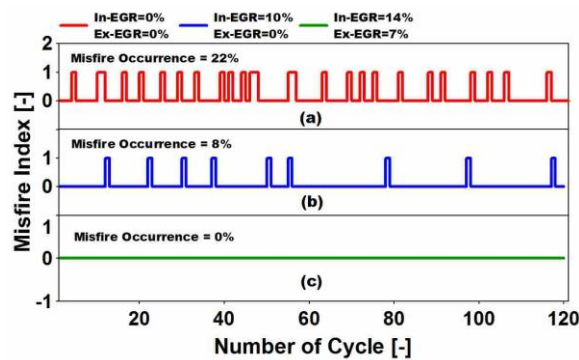
235

236

237

**Figure 3.** Influence of In-EGR and Ex-EGR on misfire occurrence at Idling condition [rpm = 1000, IMEP = 1 bar,  $T_{epc}$  = 420 K, AFR = 15]

238



239

240

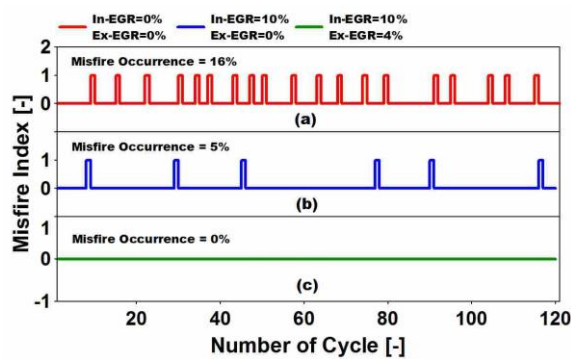
241

**Figure 4.** Influence of In-EGR and Ex-EGR on misfire occurrence at low-load condition [rpm = 2000, IMEP = 1.5 bar,  $T_{epc}$  = 431 K, AFR = 14.5]

242

Fig. 4 illustrates the influence of In/Ex-EGR utilization on the misfiring occurrence when the engine is at a higher magnitude of 2000 rpm (low-load). In general, the misfire occurrence is reduced remarkably by increasing either In-EGR or Ex-EGR. Based on Fig. 4 marking (a) shows the engine running without EGR generating 26 misfiring over 120 consecutive cycles which is 22% while, this amount has reduced to 9 cycles (misfire occurrence = 8%) when 10% of In-EGR is applied (refer Fig. 4, marking (b)). It is observed that by using a combination of both In-EGR and Ex-EGR at 14% and 7%, it will eliminate all the misfired cycles as shown in Fig. 4, marking (c). It is worth to mention that the improvement in misfire occurrence is attributed to the increment in the magnitude of  $T_{epc}$ , which is risen from 420 K to 431 K (refer Table 2).

251



252

253

254

**Figure 5.** Influence of In-EGR and Ex-EGR on misfire occurrence at mid-load condition [rpm = 3000, IMEP = 2.1 bar,  $T_{epc}$  = 451 K, AFR = 13.5]

255

256

In Fig. 5 the effect of In/Ex-EGR on misfiring occurrence is again demonstrated when the engine speed is increased to 3000 rpm (mid-load). It is can be observed that when the engine is operated at

257 a higher speed/load, having no applied In/Ex-EGR, the amount of misfire occurrence is been lowered  
 258 decreasing from 26% to 16%.

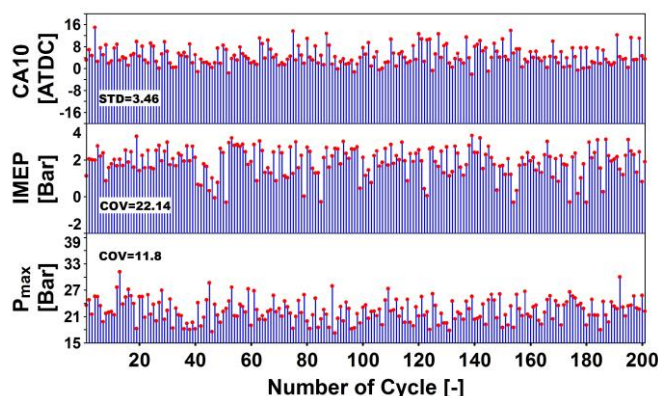
259 Similarly, the misfire phenomenon can be reduced with the combinational EGRs settings at this  
 260 engine speed. Almost 16% of the misfire occurrence (19 misfired cycles) is observed when there is no  
 261 In-EGR and Ex-EGR, as can be seen in Fig. 5 marking (a). Similarly the misfire occurrence is reduced  
 262 significantly by 5% (6 misfire cycles) when 10% of In-EGR is applied. Finally with reference to Fig. 5  
 263 marking (c), when both In-EGR and Ex-EGR are applied (at 10% and 4% respectively), the misfire  
 264 occurrence is totally eliminated. In the meantime, it can be seen that the  $T_{epc}$  is now 451 K, which is  
 265 high enough to assist in the elimination of misfire occurrence.

266 It is worth to mention that the effect of both In-EGR and Ex-EGR on misfire occurrence is  
 267 significant at lower speed operation. At lower engine rpm (especially idling), the average  
 268 temperature of in-cylinder charge is lower than when the engine is at higher engine speed (low/mid-  
 269 load). Thus, less energy is available for the mixture prior to the compression stroke. Therefore, when  
 270 the compression stroke ends, the compressed mixture temperature is still not high enough to be  
 271 ignited by the engine spark plug. In such a scenario misfire will happen. Thus, it can be generalized  
 272 that utilization of In/Ex-EGR will be more appropriate in the low engine speed and load region

## 273 7.2 Combustion Stability and Cyclic Variability Improvement

274 In order to evaluate statistically the cyclic variation of the engine combustion, parameters such  
 275 as Coefficient of variation (COV) and Standard Deviation (STD) are used. Here, in-cylinder  
 276 combustion IMEP and maximum in-cylinder pressure ( $P_{max}$ ) which are pressure-related parameters,  
 277 together with CA10 (crank angle at 10% of mass fraction burned) which is a combustion-related  
 278 parameter; are taken into consideration in an effort to examine the combustion stability when the  
 279 EGRs are applied. All data recorded for 200 consecutive cycles, which is sufficient to provide a steady  
 280 state condition for the engine during trial.

281 Fig. 6 represents the cyclic variability of CA10, IMEP and  $P_{max}$  in a conventional operation mode  
 282 wherein the engine is subjected to 3000 rpm (refer Table 2) but without EGRs. There is huge cyclic  
 283 variability for CA10, IMEP and  $P_{max}$ , which is due to poor engine combustion performance. This  
 284 shows that in such an engine operation condition the cyclic variability of the combustion is  
 285 significant. Fig. 7 presents the cyclic variability of CA10, IMEP and  $P_{max}$  when the engine is operated  
 286 at 3000 rpm by applying EGRs (In-EGR = 10 %, Ex-EGR = 4 %) as described in Table 2. Here  $COV_{IMEP}$ ,  
 287  $COV_{P_{max}}$  and  $STD_{CA10}$  are decreased significantly. The improvement in the cyclic variability of IMEP  
 288 is more considerable compared to the other parameters by reduction in  $COV_{IMEP}$  from 22.14 to 2.5.  
 289

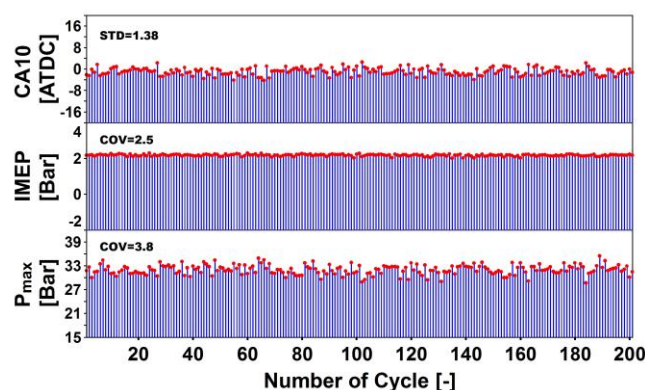


290

291 **Figure 6.** Cyclic variation of CA10, IMEP and  $P_{max}$  in conventional operation [rpm = 3000, IMEP = 2.1  
 292 bar,  $T_{epc}$  = 385 K, In-EGR = 0, Ex-EGR = 0]

293





294

295

296

**Figure 7.** Cyclic variation of CA10, IMEP and  $P_{max}$  with EGR utilization [rpm = 3000, IMEP = 2.1 bar,  $T_{epc}$  = 451 K, In-EGR = 10 %, Ex-EGR = 4 %]

297

298

299

300

301

302

303

304

305

306

307

308

309

310

311

312

313

314

315

For this part of experiment, the cyclic variation of  $P_{max}$ , CA10 and IMEP are examined in relation to In-EGR and Ex-EGR changes at 3000 rpm (mid-load), based on the operating conditions as explained in Table 3. As can be seen in Fig. 8 and Fig. 9 the utilization of In-EGR and Ex-EGR improves the cyclic variation of  $P_{max}$  ( $COV_{P_{max}}$ ) meaning that when the percentage of In-EGR and Ex-EGR increases the  $COV_{P_{max}}$  will decrease accordingly. Therefore, it can be deduced that cyclic variation of  $P_{max}$  is inversely proportional to the concentration of both In-EGR and Ex-EGR. Furthermore, it should be noted that  $P_{max}$  is more influenced by In-EGR changes since in the case of In-EGR the slope ratio for curve of fit in both Fig. 8 and Fig. 9 is more than that of Ex-EGR. The reason for this trend can be explained as: In the case of In-EGR the most dominant effect is the charge heating effect wherein both pressure and temperature at the exhaust port closure ( $P_{epc}$ ,  $T_{epc}$ ) will increase since the percentage of In-EGR is raised therefore it establishes a complete cycle of combustion. Furthermore, due to the influence of the charge heating effect and the reduction of the exhaust port area by the In-EGR valve,  $P_{epc}$  will increase extremely. Consequently,  $T_{epc}$  and heat release rate will be increased. In the case of Ex-EGR application, the most dominant effects are those of thermal and dilution effects. Utilizing Ex-EGR increases the specific heat capacity of the in-cylinder charge. However, the  $T_{epc}$  is increased slightly, the mixture takes more time to heat up. Additionally, the overall reaction rate of combustion will be suppressed due to substitute of CO<sub>2</sub> and H<sub>2</sub>O instead of O<sub>2</sub> (dilution effect) [3, 6].

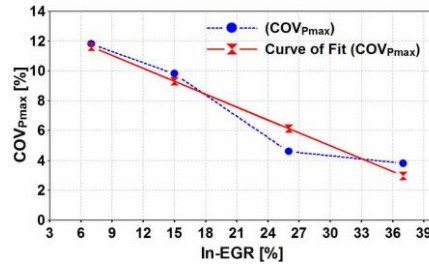
316

**Table 3.** Engine operating conditions for cyclic variability investigation

Parameters	Ranges	
	Without EGR	With EGR
Operating Condition		
Fuel [-]	Gasoline 95	Gasoline 95
Speed [rpm] ± 50	3000	3000
IMEP [bar] ± 0.1	2.1	2.1
$T_{epc}$ [K] ± 1	385	425-530
AFR [-] ± 0.5	14	14-16
$(\eta_{sc})_{ap}$ [%] ± 2	42	38-25
In-EGR [%] ± 1	0	7-37
Ex-EGR [%] ± 1	0	5-32

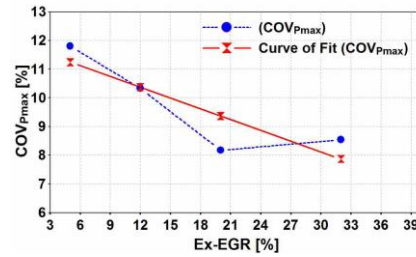
317

318



319  
320  
321

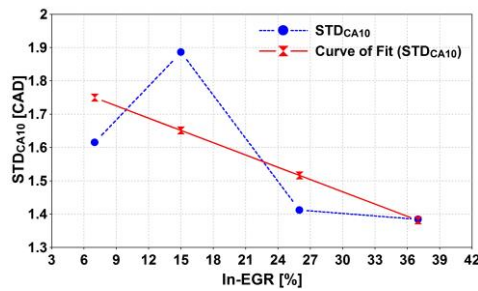
**Figure 8.** Cyclic variability of  $P_{max}$  due to variation of In-EGR setting [rpm = 3000, IMEP = 2.1 bar,  $T_{epc}$  = 425-530 K]



322  
323  
324

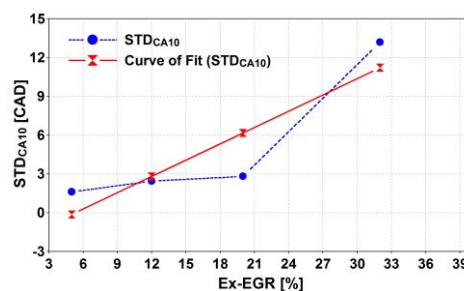
**Figure 9.** Cyclic variability of  $P_{max}$  due to variation of Ex-EGR setting [rpm = 3000, IMEP = 2.1 bar,  $T_{epc}$  = 425-530 K]

325 Fig. 10 and Fig. 11 represent the cyclic variability of CA10 ( $STD_{CA10}$ ) with respect to In-EGR and  
326 Ex-EGR variations. As illustrated in Fig. 10,  $STD_{CA10}$  decreases when In-EGR rate increases. In  
327 contrast,  $STD_{CA10}$  is increased when Ex-EGR increases. Even though In-EGR improves the cyclic  
328 variability of CA10, Ex-EGR seems to deteriorate it. Correspondingly, it is thought that  $STD_{CA10}$  is  
329 directly proportional with percentage of Ex-EGR while it is inversely proportional with the  
330 percentage of In-EGR. Furthermore, the  $STD_{CA10}$  is more sensitive to Ex-EGR changes rather than In-  
331 EGR, as it can be clearly interpreted from the slope ratio of the curves of fit in Fig. 10 and Fig. 11.  
332



333  
334  
335

**Figure 10.** Cyclic variability of CA10 with In-EGR setting [rpm = 3000, IMEP = 2.1 bar,  $T_{epc}$  = 425-530 K]



336  
337  
338

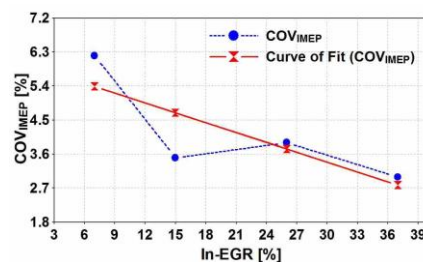
**Figure 11.** Cyclic variability of CA10 due to variation of Ex-EGR setting [rpm = 3000, IMEP = 2.1 bar,  $T_{epc}$  = 525-530 K]

339

340 The main reason for observing a contrary behaviour of  $STD_{CA10}$  in conjunction with In/Ex-EGR  
 341 can be attributed to the different dominant effect of each EGR strategies as explained earlier. The  
 342 dominant effects in In-EGR is charge-heating effect while in Ex-EGR thermal and dilution effects are  
 343 dominant. Even though the CA10 (crank angle at 10% of mass fraction burned) is basically a  
 344 combustion-related parameter, in the case of In-EGR application it tends to behaves as a pressure-  
 345 related parameter. As in Fig. 10 it can be clearly understood the  $STD_{CA10}$  is mostly affected by  
 346 increasing the in-cylinder pressure rise which caused by In-EGR application. Other words, when the  
 347 percentage of In-EGR goes up it helps to improve the  $STD_{CA10}$  since the charge heating effect and  
 348 more importantly the forced backpressure caused by exhaust port blockage (In-EGR valve closure)  
 349 are accounted for increasing in-cylinder peak pressure and temperature. Accordingly, it makes the  
 350 variation of CA10 smoothen. On the other hand, when the Ex-EGR is applied the CA10 behave as a  
 351 combustion-related parameter and the dominant effects are those which are influencing the in-  
 352 cylinder charge composition especially dilution effect which mainly supress the overall reaction rate  
 353 (heat release) in the combustion chamber. Therefore, when the Ex-EGR increases the variation of  
 354 CA10 tends to be deteriorated. It means if the Ex-EGR is applied separately it will result in a more  
 355 cyclic variability for the engine combustion which makes the instability of combustion even worse in  
 356 the higher percentage of Ex-EGR.

357 The influence of In/Ex-EGR on the cyclic variability of IMEP ( $COV_{IMEP}$ ) is illustrated in both of  
 358 Fig.12 and Fig. 13. In Fig. 12  $COV_{IMEP}$  is decreased when the In-EGR percentage is raised. But it will  
 359 become higher as Ex-EGR is increased, as shown in Fig. 13. Here it seems  $COV_{IMEP}$  is directly  
 360 proportional with change in Ex-EGR and is inversely proportional with the variation of In-EGR. The  
 361 trend indicates that  $COV_{IMEP}$  is more sensitive to the variation of Ex-EGR rather than In-EGR, as it is  
 362 can be clearly seen by examining the slope ratio of curves of fit.

363 Consequently, the major difference between In-EGR and Ex- EGR application can be inferred  
 364 that in the case of In-EGR application the charge-heating effect is more substantial since it pressurizes  
 365 the combustion chamber significantly, which leads to higher  $P_{epc}$  and  $T_{epc}$ . Even though in-cylinder  
 366 charge composition will change (due to thermal and dilution effects) with In-EGR, it is not significant  
 367 as compared to changes in  $T_{epc}$ , which is more substantial. In contrast, Ex-EGR will just mix burned  
 368 gases to the intake charge leading to changes in in-cylinder charge composition and temperature. In  
 369 this case the increase in the mixture temperature  $T_{epc}$  will not be considerable while the effect of  
 370 changes in specific heats (thermal effect) and lack of oxygen (dilution effect) will be important  
 371 significantly [3, 6].

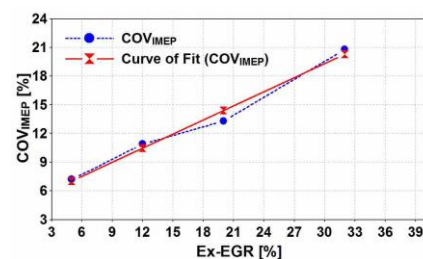


372

373

374

**Figure 12.** Cyclic variability of IMEP due to variation of In-EGR setting [rpm = 3000, IMEP = 2.1 bar,  $T_{epc} = 525\text{-}530$  K]



375

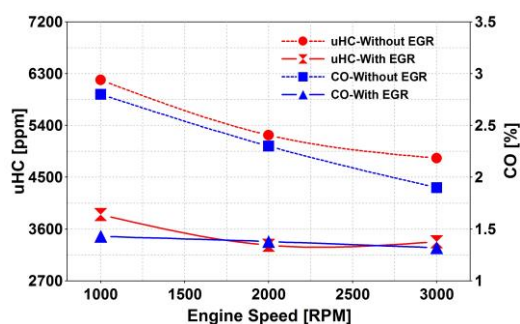
376

377

**Figure 13.** Cyclic variability of IMEP due to variation of Ex-EGR setting [rpm = 3000, IMEP = 2.1 bar,  $T_{epc} = 525\text{-}530$  K]

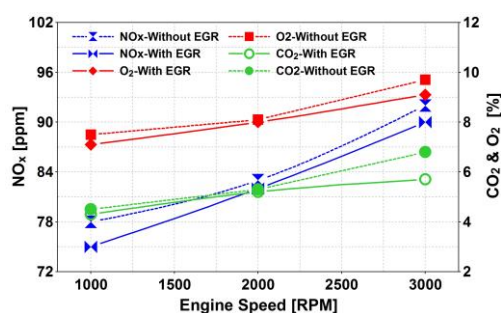
### 378 7.3 Idling, Low-Load and Mid-Load Emissions Improvement

379 In order to examine for the engine exhaust emissions characteristics, it is run at three speeds  
 380 including 1000 rpm (idling), 2000 rpm (low-load) and 3000 rpm (mid-load) corresponding as  
 381 identically same as aforementioned section test point conditions (refer Table 2). The exhaust gas  
 382 concentrations are measured in two states of the engine operation condition. Firstly the state as such  
 383 a conventional engine operation (without EGR) and secondly the state with application of EGR  
 384 (combined effect of In/Ex-EGR, refer Table 2). For each of these states the engine is operated in three  
 385 different speeds (1000, 2000 and 3000 rpm)  
 386



387  
 388 **Figure 14.** Influence of In/Ex-EGR on uHC and CO concentrations at idling and low/mid-load settings  
 389 [rpm = 1000-3000, IMEP = 1-2.1 bar,  $T_{epc}$  = 385-530 K, AFR = 14-16]

390 Fig. 14 represents the variation of uHC and CO emissions against engine speed before and after  
 391 EGR application. The concentration of both uHC and CO is lowered when EGR applied. From the  
 392 trend shown it can be interpreted that rate of variations in uHC and CO concentration decrease with  
 393 the increased in speed. However, engine speed does not impair significantly on the emission  
 394 concentration of CO when the EGRs are applied. As discussed earlier, since the incomplete  
 395 combustion cycles (i.e. misfire cycle) are eliminated, due to the using of In/Ex-EGR, the exhaust  
 396 constituents such as uHC and CO are subjected to change. Having an improved combustion  
 397 (completed combustion) will result in lower concentration of uHC and CO.  
 398



399  
 400 **Figure 15.** Influence of In/Ex-EGR on NO<sub>x</sub>, CO<sub>2</sub> and O<sub>2</sub> concentrations at idling and low/mid-load  
 401 settings [rpm = 1000-3000, IMEP = 1-2.1 bar,  $T_{epc}$  = 385-530 K, AFR = 14-16]

402 Fig. 15 presents the variation of NO<sub>x</sub>, CO<sub>2</sub> and O<sub>2</sub> emissions against the speed before and after  
 403 EGR is applied. From the results the concentrations of NO<sub>x</sub>, CO<sub>2</sub> and O<sub>2</sub> decrease for all three speeds,  
 404 however the improvements do not follow the trend as observed earlier for uHC and CO. From the of  
 405 exhaust emission the EGR application for this type of engine at idling, low-load and mid-load regions  
 406 mainly affect the reduction in the concentration of uHC and CO, more than that of NO<sub>x</sub>, CO<sub>2</sub> and O<sub>2</sub>.

### 407 8. Conclusion

408 An experimental study was conducted to investigate the influence of In-EGR and Ex-EGR on the  
 409 combustion parameters of a spark ignition two-stroke cycle engine for which combustion cyclic

410 variability, misfire occurrence and exhaust emissions were examined. The outcomes of the  
411 investigation are summarized as follows:

412

- 413 • The overall effect of EGR is to increase the cylinder charge temperature, which has proven to  
414 produce higher exhaust port closure temperature ( $T_{epc}$ ) resulting in lower misfiring cycles.
- 415 • Reduction in the misfire occurrence due to EGR is apparent at the engine's lower engine speed  
416 region.
- 417 • As for average charge temperature ( $T_{epc}$ ), In-EGR is more effective than Ex-EGR. It not only  
418 increases the  $T_{epc}$  but also increase the pressure of cylinder at the start of combustion ( $P_{epc}$ ).
- 419 • Both In-EGR and Ex-EGR improve the cyclic variability of the combustion parameters,  
420 specifically the IMEP.
- 421 • The cyclic variability of CA10, IMEP and  $P_{max}$  will be further improved by applying In-EGR.  
422 Ex-EGR will impair cyclic variability of CA10, IMEP but will improve  $P_{max}$ .
- 423 • The application of EGR offers a significant means to improve and eliminate low and mid load  
424 misfire combustion of spark ignition two-stroke cycle engine leading to emission reduction.

425

#### 426 **Acknowledgments:**

427 The authors would like to acknowledge the Universiti Teknologi Malaysia (UTM) for financial  
428 support under the research university grant Q.J130000.3509.06G97.

429

#### 430 **Author Contributions:**

431 Amin Mahmoudzadeh Andwari, has written the paper context and performed the experimental  
432 work alongside results presentation. Apostolos Pesyridis, Vahid Esfahanian and Mohd Farid  
433 Muhamad Said have carried out the design of experiment in the simulation.

434

435 **Conflicts of Interest:** The authors declare no conflict of interest.

#### 436 **References**

- 437 1. Benajes, J.; Novella, R.; De Lima, D.; Tribotté, P.; Quechon, N.; Obernesser, P.; Dugue, V., Analysis of  
438 the combustion process, pollutant emissions and efficiency of an innovative 2-stroke HSDI engine  
439 designed for automotive applications. *Applied Thermal Engineering* **2013**, *58*, (1–2), 181-193.
- 440 2. Duret, P., *A New Generation of Engine Combustion Processes for the Future?: Proceedings of the International*  
441 *Congress, Held in Rueil-Malmaison, France, November, 26-27, 2001*. Editions Technip: 2002.
- 442 3. Mahmoudzadeh Andwari, A.; Abdul Aziz, A.; Muhamad Said, M. F.; Abdul Latiff, Z., An experimental  
443 study on the influence of EGR rate and fuel octane number on the combustion characteristics of a CAI  
444 two-stroke cycle engine. *Applied Thermal Engineering* **2014**, *71*, (1), 248-258.
- 445 4. Ishibashi, Y., Basic Understanding of Activated Radical Combustion and Its Two-Stroke Engine  
446 Application and Benefits. *SAE Paper 2000-01-1836* **2000**.
- 447 5. Mahmoudzadeh Andwari, A.; Aziz, A. A.; Said, M. F. M.; Esfahanian, V.; Latiff, Z. A.; Said, S. N. M.,  
448 Effect of internal and external EGR on cyclic variability and emissions of a spark ignition two-stroke  
449 cycle gasoline engine. *Journal of Mechanical Engineering and Sciences* **2017**, *11*, (4), 3004-3014.
- 450 6. Mahmoudzadeh Andwari, A.; Aziz, A. A.; Said, M. F. M.; Latiff, Z. A., Experimental investigation of  
451 the influence of internal and external EGR on the combustion characteristics of a controlled auto-  
452 ignition two-stroke cycle engine. *Applied Energy* **2014**, *134*, 1-10.
- 453 7. Zhao, H., *HCCI and CAI engines for the automotive industry*. Woodhead Pub.: 2007.
- 454 8. Zhao, H.; Ladommatos, N., Engine combustion instrumentation and diagnostics. *Warrendale, PA:*  
455 *Society of Automotive Engineers, 2001*. 842 **2001**.
- 456 9. Asai, M.; Kurosaki, T.; Okada, K., Analysis on Fuel Economy Improvement and Exhaust Emission  
457 Reduction in a Two-Stroke Engine by Using an Exhaust Valve. *SAE Paper 951764* **1995**.
- 458 10. Blair, G. P.; Kenny, R. G., Further Developments in Scavenging Analysis for Two-Cycle Engines. In *SAE*  
459 *International: 1980*.
- 460 11. Fang, Q.; Fang, J.; Zhuang, J.; Huang, Z., Influences of pilot injection and exhaust gas recirculation  
461 (EGR) on combustion and emissions in a HCCI-DI combustion engine. *Applied Thermal Engineering*  
462 **2012**, *48*, (0), 97-104.

- 463 12. Mahmoudzadeh Andwari, A.; Azhar, A. A., Homogenous Charge Compression Ignition (HCCI)  
464 Technique: A Review for Application in Two-Stroke Gasoline Engines. *Applied Mechanics and Materials*  
465 **2012**, 165, 53-57.
- 466 13. Mahmoudzadeh Andwari, A.; Aziz, A. A.; Muhamad Said, M. F.; Abdul Latiff, Z., Controlled Auto-  
467 Ignition Combustion in a Two-Stroke Cycle Engine Using Hot Burned Gases. *Applied Mechanics and*  
468 *Materials* **2013**, 388, 201-205.
- 469 14. Mahmoudzadeh Andwari, A.; Pesiridis, A.; Esfahanian, V.; Salavati-Zadeh, A.; Karvountzis-  
470 Kontakiotis, A.; Muralidharan, V., A Comparative Study of the Effect of Turbocompounding and ORC  
471 Waste Heat Recovery Systems on the Performance of a Turbocharged Heavy-Duty Diesel Engine.  
472 *Energies* **2017**, 10, (8), 1087.
- 473 15. Blair, G. P., *The Basic Design of Two-stroke Engines*. Society of Automotive Engineers: 1990.
- 474 16. Duret, P., *A New Generation of Two-stroke Engines for the Future?: Proceedings of the International Seminar*  
475 *Held in Rueil-Malmaison, France, November 29-30, 1993*. Éditions Technip: 1993.
- 476 17. Duret, P.; Moreau, J.-F., Reduction of Pollutant Emissions of the IAPAC Two-Stroke Engine with  
477 Compressed Air Assisted Fuel Injection. *SAE Paper 900801* **1990**.
- 478 18. Ishibashi, Y.; Asai, M., Improving the Exhaust Emissions of Two-Stroke Engines by Applying the  
479 Activated Radical Combustion. *SAE Paper 960742* **1996**.
- 480 19. Mahmoudzadeh Andwari, A.; Aziz, A. A.; Said, M. F. M.; Latiff, Z. A., A Converted Two-Stroke Cycle  
481 Engine for Compression Ignition Combustion. *Applied Mechanics and Materials* **2014**, 663, 331-335.
- 482 20. Mahmoudzadeh Andwari, A.; Aziz, A. A.; Said, M. F. M.; Latiff, Z. A.; Ghanaati, A., Influence Of Hot  
483 Burned Gas Utilization On The Exhaust Emission Characteristics Of A Controlled Auto-Ignition Two-  
484 Stroke Cycle Engine. *International Journal of Automotive and Mechanical EngineeringOnline* **2015**, 11, 2229-  
485 8649.
- 486 21. Mahmoudzadeh Andwari, A.; Pesiridis, A.; Karvountzis-Kontakiotis, A.; Esfahanian, V., Hybrid  
487 electric vehicle performance with organic rankine cycle waste heat recovery system. *Appl. Sci.* **2017**, 7,  
488 (5).
- 489 22. Nishi, M.; Kanehara, M.; Iida, N., Assessment for innovative combustion on HCCI engine by controlling  
490 EGR ratio and engine speed. *Applied Thermal Engineering* **2016**, 99, 42-60.
- 491 23. Nishida, K.; Sakuyama, H.; Kimijima, T., Improvement of Fuel Economy Using a New Concept of Two-  
492 Stroke Gasoline Engine Applying Stratified-Charge Auto-Ignition. In *The Automotive Research*  
493 *Association of India: 2009*.
- 494 24. Noguchi, M.; Tanaka, Y.; Tanaka, T.; Takeuchi, Y., A Study on Gasoline Engine Combustion by  
495 Observation of Intermediate Reactive Products during Combustion. *SAE Paper 790840* **1979**.
- 496 25. Onishi, S.; Jo, S. H.; Shoda, K.; Jo, P. D.; Kato, S., Active Thermo-Atmosphere Combustion (ATAC) - A  
497 New Combustion Process for Internal Combustion Engines. *SAE Paper 790501* **1979**.
- 498 26. Ozdor, N.; Dulger, M.; Sher, E., Cyclic Variability in Spark Ignition Engines A Literature Survey. In *SAE*  
499 *International: 1994*.
- 500 27. Salvi, B. L.; Subramanian, K. A., Experimental investigation on effects of exhaust gas recirculation on  
501 flame kernel growth rate in a hydrogen fuelled spark ignition engine. *Applied Thermal Engineering* **2016**,  
502 107, 48-54.
- 503 28. Takei, T.; Iida, N., Study on Auto-Ignition and Combustion Completion of n-Butane in a Two-stroke  
504 Homogeneous Charge Compression Ignition (HCCI) Engine. **2002**.
- 505 29. Yao, M.; Zheng, Z.; Liu, H., Progress and recent trends in homogeneous charge compression ignition  
506 (HCCI) engines. *Progress in Energy and Combustion Science* **2009**, 35, (5), 398-437.
- 507 30. Zhang, Y.; Zhao, H.; Ojapah, M.; Cairns, A., CAI combustion of gasoline and its mixture with ethanol  
508 in a 2-stroke poppet valve DI gasoline engine. *Fuel* **2013**, 109, (0), 661-668.
- 509 31. Yu, X.; Wu, H.; Du, Y.; Tang, Y.; Liu, L.; Niu, R., Research on cycle-by-cycle variations of an SI engine  
510 with hydrogen direct injection under lean burn conditions. *Applied Thermal Engineering* **2016**, 109, Part  
511 A, 569-581.
- 512 32. Mahmoudzadeh Andwari, A.; Said, M. F. M.; Aziz, A. A.; Esfahanian, V.; Salavati-Zadeh, A.; Idris, M.  
513 A.; Perang, M. R. M.; Jamil, H. M., Design, Modeling and Simulation of a High-Pressure Gasoline Direct  
514 Injection (GDI) Pump for Small Engine Applications. *Journal of Mechanical Engineering (JMchE)* **2018**, SI  
515 6, (1), 107-120.
- 516 33. Mahmoudzadeh Andwari, A.; Said, M. F. M.; Aziz, A. A.; Esfahanian, V.; Baker, M. R. A.; Perang, M.  
517 R. M.; Jamil, H. M., A Study on Gasoline Direct Injection (GDI) Pump System Performance using Model-  
518 Based Simulation. *Journal of Society of Automotive Engineers Malaysia (jsAEM)* **2018**, 2, (1), 14-22.
- 519 34. Iida, N.; Yamasaki, Y.; Sato, S.; Kumano, K.; Kojima, Y., Study on Auto-Ignition and Combustion  
520 Mechanism of HCCI Engine. *SAE Paper 2004-32-0095* **2004**.

- 521 35. Heywood, J. B.; Sher, E.; Engineers, S. o. A., *The Two-Stroke Cycle Engine: Its Development, Operation, and*  
522 *Design*. Taylor & Francis: 1999.
- 523 36. Zhang, Y.; Zhao, H.; Ojapah, M.; Cairns, A., Experiment and Analysis of a Direct Injection Gasoline  
524 Engine Operating with 2-stroke and 4-stroke Cycles of Spark Ignition and Controlled Auto-Ignition  
525 Combustion. In SAE International: 2011.
- 526 37. Karvountzis-Kontakiotis, A.; Mahmoudzadeh Andwari, A.; Pesyridis, A.; Russo, S.; Tuccillo, R.;  
527 Esfahanian, V., Application of Micro Gas Turbine in Range-Extended Electric Vehicles. *Energy* **2018**,  
528 147, 351-361.
- 529 38. Iida, N., Combustion Analysis of Methanol-Fueled Active Thermo-Atmosphere Combustion (ATAC)  
530 Engine Using a Spectroscopic Observation. *SAE Paper 940684* **1994**.
- 531 39. Heywood, J. B., *Internal combustion engine fundamentals*. McGraw-Hill: 1988.
- 532 40. Ghanaati, A.; Mat Darus, I. Z.; Farid, M.; Said, M.; Mahmoudzadeh Andwari, A., A Mean Value Model  
533 For Estimation Of Laminar And Turbulent Flame Speed In Spark-Ignition Engine. *International Journal*  
534 *of Automotive and Mechanical EngineeringOnline* **2015**, 11, 2229-8649.
- 535 41. Blair, G. P.; Committee, S. P. A. S. P., *Advances in Two-Stroke Cycle Engine Technology*. Society of  
536 Automotive Engineers: 1989.
- 537 42. Nuti, M.; Martorano, L., Short-Circuit Ratio Evaluation in the Scavenging of Two-Stroke S.I. Engines.  
538 In SAE International: 1985.
- 539 43. Tsuchiya, K.; Hirano, S.; Okamura, M.; Gotoh, T., Emission Control of Two-Stroke Motorcycle Engines  
540 by the Butterfly Exhaust Valve. *SAE Paper 800973* **1980**.
- 541 44. Iijima, A.; Yoshida, K.; Shoji, H., A Comparative Study of HCCI and ATAC Combustion Characteristics  
542 Based on Experimentation and Simulations Influence of the Fuel Octane Number and Internal EGR on  
543 Combustion. In SAE International: 2005.
- 544 45. Liu, H.; Zhang, P.; Li, Z.; Luo, J.; Zheng, Z.; Yao, M., Effects of temperature inhomogeneities on the  
545 HCCI combustion in an optical engine. *Applied Thermal Engineering* **2011**, 31, (14–15), 2549-2555.
- 546 46. Goto, K.; Iijima, A.; Yoshida, K.; Shoji, H., Analysis of the Characteristics of HCCI Combustion and  
547 ATAC Combustion Using the Same Test Engine. In SAE International: 2004.
- 548 47. García, M. T.; Aguilar, F. J. J.-E.; Lencero, T. S.; Villanueva, J. A. B., A new heat release rate (HRR) law  
549 for homogeneous charge compression ignition (HCCI) combustion mode. *Applied Thermal Engineering*  
550 **2009**, 29, (17–18), 3654-3662.
- 551 48. Duret, P.; Ecomard, A.; Audinet, M., A New Two-Stroke Engine with Compressed-Air Assisted Fuel  
552 Injection for High Efficiency low Emissions Applications. *SAE Paper 880176* **1988**.
- 553 49. Zhang, Y.; Zhao, H.; Ojapah, M.; Cairns, A., Effects of Injection Timing on CAI Operation in a 2/4-Stroke  
554 Switchable GDI Engine. *SAE Int. J. Engines* **2011**, 5, (2), 67-75.
- 555 50. Liu, Y.; Zhang, F.; Zhao, Z.; Dong, Y.; Ma, F.; Zhang, S., Study on the synthetic scavenging model  
556 validation method of opposed-piston two-stroke diesel engine. *Applied Thermal Engineering* **2016**, 104,  
557 184-192.
- 558 51. Ishibashi, Y.; Asai, M., A Low Pressure Pneumatic Direct Injection Two-Stroke Engine by Activated  
559 Radical Combustion Concept. *SAE Paper 980757* **1998**.
- 560 52. Duret, P.; Venturi, S. p., Automotive Calibration of the IAPAC Fluid Dynamically Controlled Two-  
561 Stroke Combustion Process. *SAE Paper 960363* **1996**.
- 562 53. Duret, P.; Dabadie, J.-C.; Lavy, J.; Allen, J.; Blundell, D.; Oscarsson, J.; Emanuelsson, G.; Perotti, M.;  
563 Kenny, R.; Cunningham, G., The Air Assisted Direct Injection ELEVATE Automotive Engine  
564 Combustion System. *SAE Paper 2000-01-1899* **2000**.
- 565  
566  
567

568	<b>Glossary</b>
569	a/bTDC after/before top dead center
570	AFR engine air-to-fuel ratio center
571	CO <sub>2</sub> carbon dioxide
572	COV coefficient of variation
573	CA10 crank angle at 10% of mass fraction burned
574	Ex-EGR external exhaust gas recirculation
575	HCCI homogeneous charge compression ignition
576	IMEP indicated mean effective pressure
577	In-EGR internal exhaust gas recirculation
578	$K_0, K_1, K_2$ scavenging coefficients
579	$k$ heat capacity ratio
580	$L_{ap}$ applied corrected delivery ratio
581	$L_{inh}$ inherent corrected delivery ratio
582	$\dot{m}^{fuel}$ fuel mass flow rate
583	$M_{del}$ mass of fresh charge delivered
584	$M_{tr}$ mass of total gas trapped
585	NO <sub>x</sub> nitric oxides
586	$N_s$ engine speed in RPM
587	NTC negative temperature coefficient
588	$P_{epc}$ in-cylinder pressure at exhaust port closure
589	$P_{max}$ maximum in-cylinder pressure
590	STD standard deviation
591	$R$ specific gas constant
592	$T_{ex}$ exhaust gas temperature
593	$T_{epc}$ in-cylinder gas temperature at exhaust port closure
594	$T_{epo}$ in-cylinder gas temperature at exhaust port opening
595	$T_{sc}$ scavenging gas temperature
596	$T_r$ residual gas temperature
597	uHC unburned hydrocarbon
598	$V_{epc}$ sweep volume at exhaust port closure
599	$\gamma_{inh}$ inherent residual gas ratio
600	$\gamma_{ap}$ applied residual gas ratio
601	$(\eta_{sc})_{inh}$ inherent scavenging efficiency
602	$(\eta_{sc})_{ap}$ applied scavenging efficiency
603	
604	
605	